13th FIG Symposium on Deformation Measurement and Analysis
4th IAG Symposium on Geodesy for Geotechnical and Structural Engineering

LNEC, LISBON 2008 May 12-15

SMOOTHING GNSS TIME SERIES WITH ASYMMETRIC SIMPLE MOVING AVERAGES

José Nuno LIMA, and João CASACA

National Laboratory for Civil Engineering, Portugal[1]

Abstract: There is an increasing trend to apply GNSS continuous observation of short baselines to the monitoring of engineering works, such as bridges and dams, for their structural analysis and safety control. In the case of large dams, one important application of the GNSS continuous observation is the establishment of early warning systems that demand accurate, frequently updated information and where the analysis of the baseline time series, in order to separate signal from noise is mandatory. The paper presents a study on the performance of linear filters of the asymmetric moving average type to smooth baseline time series. The transfer function of the filter is adopted as a smoothing criterion to choose an adequate order for the moving average, in face of the spectral density function of the baseline time series. One series of measurements of a short test baseline (325 m), materialised in the campus of the National Laboratory for Civil Engineering, is used as an example of the proposed strategy.

1. INTRODUCTION

The continuous observation of short baseline vectors defined by permanent GNSS stations has been increasingly applied to the monitoring of engineering works, such as bridges, buildings and dams, for structural analysis with safety control purposes. The sampling frequency and the processing frequency of the phase observations must be adjusted to the type of work: the monitoring of a bridge, due to the vibrations caused by the wind and vehicle loading, needs a much higher processing frequency than the monitoring of a dam, unless seismic actions are to be taken into account.

The use of GNSS permanent stations with continuous observation in warning systems of large engineering works requires, on one hand, short processing intervals, and on the other hand, real time high quality results. The asymmetric filters of the simple moving average type, that act as low-pass filters, appear to be one solution to the problem. The paper presents a study on the properties of this type of filters, in particular, on the performance of their gain and phase shift functions.

The concepts are applied to a time series resulting from the observation of a short (325m) test baseline temporarily materialized in the campus of the National Laboratory for Civil Engineering (NLCE), over three days. The observations were carried out with two TOPCON dual frequency GNSS receivers with choke-ring antennae and processed with the PINNACLE software. The measurements were carried out with a sampling frequency of 0.2Hz and the processing interval was five minutes.

2. LINEAR FILTERS, GAIN AND PHASE SHIFT

A linear combination of the terms of a time series ($x_0,x_1,...,x_n$):

$$y_k = \sum_{j=-q}^{r} w_j x_{k+j} \quad (k = q+1,\ldots,n-r) \tag{1}$$

where the m (= q + r + 1) coefficients w_j are called weights, is said to be a linear filter of order m. If q = r and $w_j = w_{-j}$, the filter is said to be symmetric. If the weights sum up to one, the filter is called a weighted moving average. If the weights are equal and sum up to one, the filter is called a simple moving average.

The application of a filter to a time series (the input time series ($x_0,x_1,...,x_n$)) produces a new time series (the output time series ($y_0,y_1,...,y_n$)). The spectral characteristics of the output series are related to the spectral characteristics of the input series by means of the transfer function of the filter. The transfer function is a complex function with arguments in the frequency domain. The modulus of the transfer function is called the gain of the filter. The argument of the transfer function is called the phase shift of the filter.

If the gain of the filter, for a given angular frequency (ω), is greater than one, the filter amplifies the input series in that frequency. Otherwise, if the gain of the filter, for (ω), is lesser than one, the filter softens the input series in that frequency.

Besides the change in amplitude the filter may also introduce a phase shift on the output time series depending on the frequency. Though the symmetric filters do not introduce significant phase shifts, the asymmetric ones do.

3. THE ASYMMETRIC SIMPLE MOVING AVERAGES

The asymmetric simple moving averages (ASMA) of order m (= q+1), which have constant weights ($w_j = m^{-1}$), may be expressed as:

$$y_k = \frac{1}{m} \sum_{j=-q}^{0} x_{k+j} \quad (k = q+1,\ldots,n) \tag{2}$$

The gain function of an ASMA filter of order m (= q+1) is:

$$g(\omega) = \frac{1}{m}\sqrt{\left(\sum_{k=-q}^{0} cos(k\omega)\right)^2 + \left(\sum_{k=-q}^{0} sin(k\omega)\right)^2} \tag{3}$$

Figure 1 presents the graphics of the gain function for ASMA filters of orders m = 6, 12, 24, 36 and 48. The (dimensionless) values of the gain functions are plotted against periods from 24h to 0h. The Figure shows that all these filters are low-pass filters. The 48th order ASMA filter begins to reduce the amplitudes at lower frequencies, i. e., at higher periods, than the 36th order ASMA filter, and so on. The 6th order ASMA is the more permissive filter to high frequencies, i. e., to low periods.

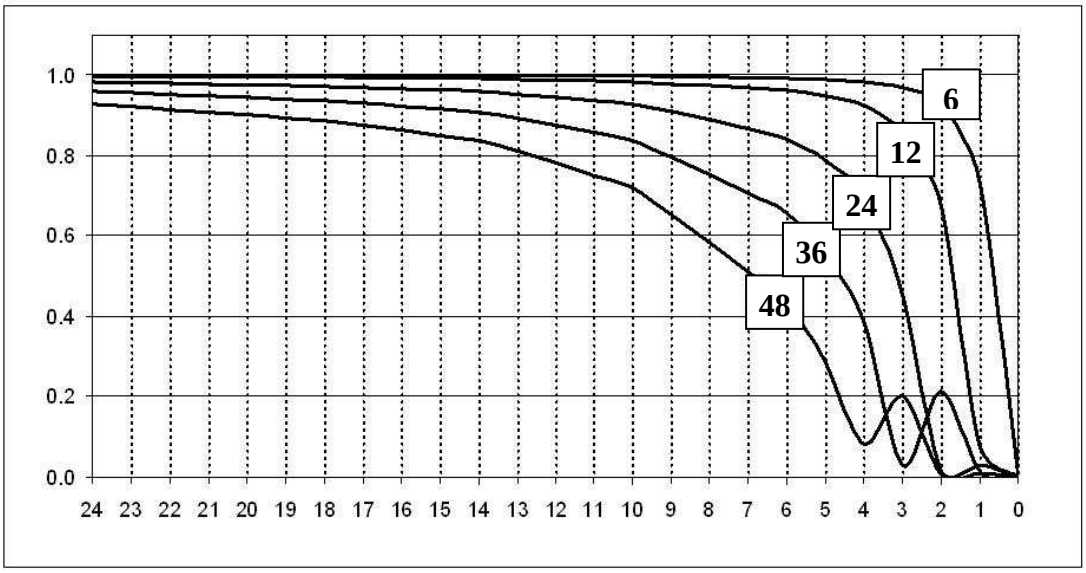

Figure 1 – The gain function of ASMA filters of order 6, 12, 24, 36 and 48. The periods, in the x-axis, are in hours. The gains, in the y-axis, are dimensionless.

The phase-shift function of a filter originates a time delay (τ) in the output (filtered) time series. The phase-shift of an ASMA filter of order m (= q+1) is:

$$\phi(\omega) = arctan\left(\frac{\sum_{k=-q}^{0} sin(k\,\omega)}{\sum_{k=-q}^{0} cos(k\,\omega)} \right) \tag{4}$$

The time delay originated by the phase-shift is given by:

$$\tau = \frac{\phi}{\omega} = \frac{\phi}{2\pi} p \tag{5}$$

where p is the period.

Figure 2 presents the graphics of the phase-shift function for ASMA filters of orders m = 6, 12, 24, 36 and 48. The values of the phase-shift function are plotted for the frequencies correspondent to periods between 24h and 0h. The Figure shows that, for the same period, the phase-shift increases with the order of the ASMA filter.

According to the Figure 2, for a semi-diurnal wave, the 6th order ASMA filter suffers a phase-shift of 20º, which corresponds to a 40 minutes time delay, and the 48th order ASMA filter suffers a phase shift of 180º, which corresponds to a 6 hour delay. The time delay of a high order ASMA filter may overcome the benefit of its smoothing properties.

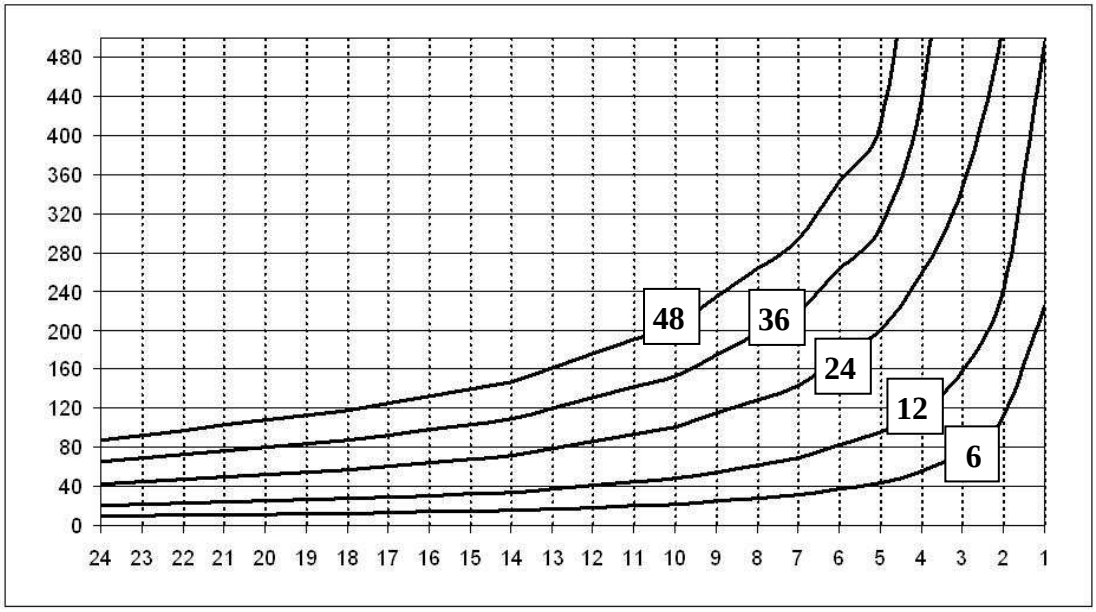

Figure 2 – The phase-shift of ASMA filters of order 6, 12, 24, 36 and 48. The periods, in the x-axis, are in hours. The phase-shifts, in the y-axis, are in degrees.

4. THE PERIODOGRAM

Let x(t) to be a continuous real function defined in the time interval [0, T], which values:

$$x_0 = x(t_0), x_1 = (t_1), x_2 = x(t_2), \ldots, x_n = x(t_{n-1}) \tag{6}$$

are known (or measured) on n equally spaced epochs (t_k), such that the (constant) sampling interval Δt verifies:

$$(n-1)\Delta t = T \tag{7}$$

The function x(t) may be expanded in a finite Fourier series in the time interval [0, T] (Schureman, 1941):

$$x(t) = \sum_{k=0}^{r} a_k \cos(\omega_k t) + \sum_{k=0}^{s} b_k \sin(\omega_k t) \tag{8}$$

where: i) r = n/2 and s = r – 1, if n is even; ii) r = s= (n – 1)/2, if n is odd. The angular frequencies of the Fourier series (8) are:

$$\omega_0 = 0, \omega_1 = 2\pi\frac{1}{T}, \omega_2 = 2\pi\frac{2}{T}, \ldots, \omega_r = 2\pi\frac{r}{T}, \tag{9}$$

The periodogram of the time series is the graphic of the spectral density function:

$$c_k = \sqrt{a_k^2 + b_k^2} \quad (k = 1, \ldots, n-1) \tag{10}$$

plotted as a function of the periods (p_k = T/k). The maximum values of the periodogram (10) are attained at the periods of order k with the most significant amplitudes (a_k, b_k, c_k).

5. THE TEST BASELINE

A short baseline (325m), materialized temporarily at the campus of the NLCE, was observed continuously over three days, beginning at 0h of the first day. The observations were carried out, with a sampling frequency of 0.2Hz, using two dual frequency GNSS receivers and choke-ring antennae from TOPCON. The carrier phase observations were processed with five minute intervals.

A time series of 863 baseline vectors was obtained. The Cartesian components (x, y, z) were transformed to the topocentric components: North-South (N), East-West (E) and Up-Down (U). The topocentric *components* measured in the first epoch were subtracted from all the others, originating three new series of 862 topocentric component changes (dN, dE, dU).

Fourier expansions in the interval [0, T = 3 days] were carried out for the two time series of the topocentric component changes (dN and dE), in order to compute the spectral density functions and draw the correspondent periodograms. Figure 3 presents the periodogram of the observed North-South component changes (dN) for periods between three days (72 hours) and 10 minutes (the Nyquist frequency). The Figure shows that the most significant values are in the range of the higher periods (lower frequencies).

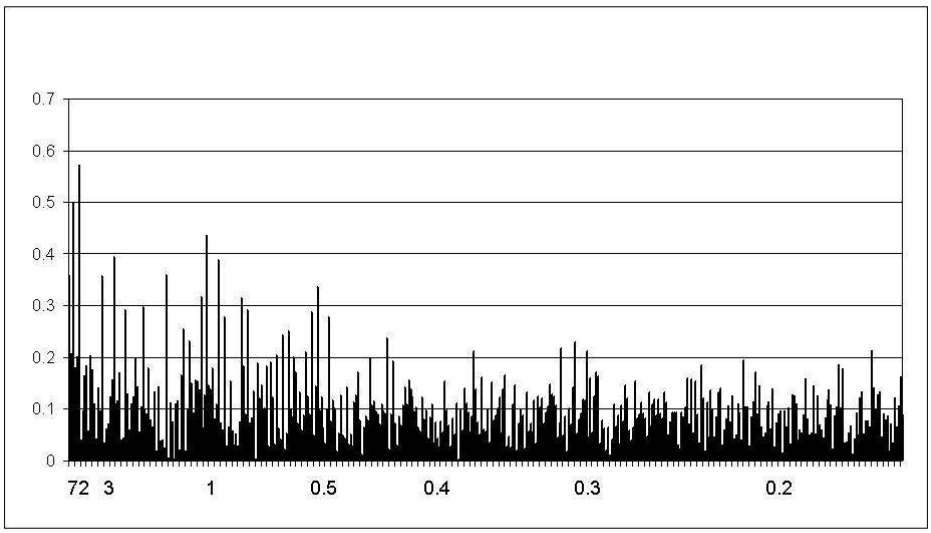

Figure 3 – Periodogram of the observed North-South component changes (dN) time series. The periods, in the x-axis, are in hours (the scale is not uniform). The amplitudes, in the y-axis, are in mm.

The two time series of North-South (dN) and East-West (dE) component changes were processed with a 12^{th} order ASMA filter. The two output time series (dN_{12} and (dE_{12}) were expanded in a finite Fourier series in the same interval [0, T = 3days]. The resulting periodogram for the (dN_{12}) time series is presented at the Figure 4. The comparative analysis of the periodograms of the Figures 3 and 4 shows the effect of the 12^{th} order ASMA filter. The higher frequencies (lower periods, bellow two hours) were almost annihilated by the filter.

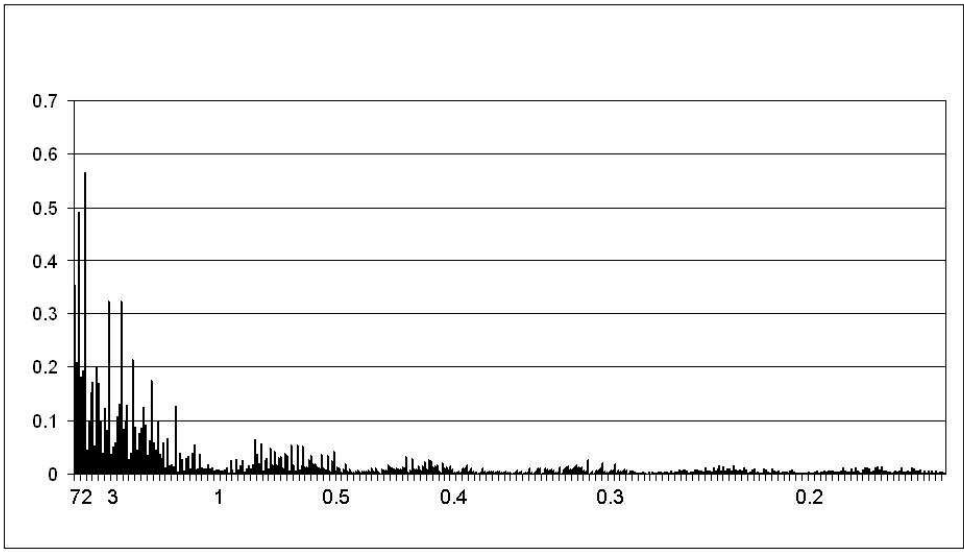

Figure 4 – Periodogram of the North-South component changes (dN) time series, after filtering with a 12th order ASMA. The periods, in the x-axis, are in hours (the scale is not uniform). The amplitudes, in the y-axis, are in mm.

To quantify the visual comparison of the Figures 3 and 4, the Table 1 presents the five highest values of the spectral density functions (c) of the dN and dE time series (before filtering) as well as the correspondent values of the spectral density functions (c_{12}) of the time series dN and dE (after filtering) and the correspondent periods (in hours). The table shows that the amplitudes that correspond to the larger periods remain unchanged though the amplitudes that correspond to the smaller periods are significantly reduced.

Table 1 – Maximum values of the spectral density function and the correspondent periods

dN			dE		
period	**c**	**c_{12}**	**period**	**c**	**c_{12}**
12.00 h	0.573 mm	0.565 mm	12.00 h	0.327 mm	0.324 mm
24.00 h	0.499 mm	0.491 mm	00.75 h	0.321 mm	0.070 mm
01.00 h	0.437 mm	0.007 mm	01.30 h	0.296 mm	0.091 mm
03.00 h	0.395 mm	0.324 mm	02.00 h	0.265 mm	0.169 mm
00.92 h	0.389 mm	0.024 mm	00.56 h	0.262 mm	0.031 mm

According to the Table 1, in both cases of the dN and the dE time series, the amplitude of the dominant harmonic, which is a semi-diurnal harmonic, is not affected by the 12th order ASMA filter. In the case of the dN time series, the amplitude of the second dominant harmonic, which is a diurnal harmonic, is not also affected by the filter.

6. SMOOTHING THE OBSERVED TIME SERIES

The spectral decomposition may be used to smooth the observed time series (dN, dE, dU). The Figure 4 presents the graphic of the observed (dN) time series and the graphic of its

reconstruction with a composition of the four more significant frequencies: the semidiurnal, the diurnal, etc. (see Table 1). The Figure also presents the result of the application of a 12th order ASMA filter to the observed (dN) time series. A quick look to the graphics shows that the spectral composition reduces the variability of the data roughly to a ±2 mm band, while the 12th order ASMA filter has a slightly worse performance in this domain.

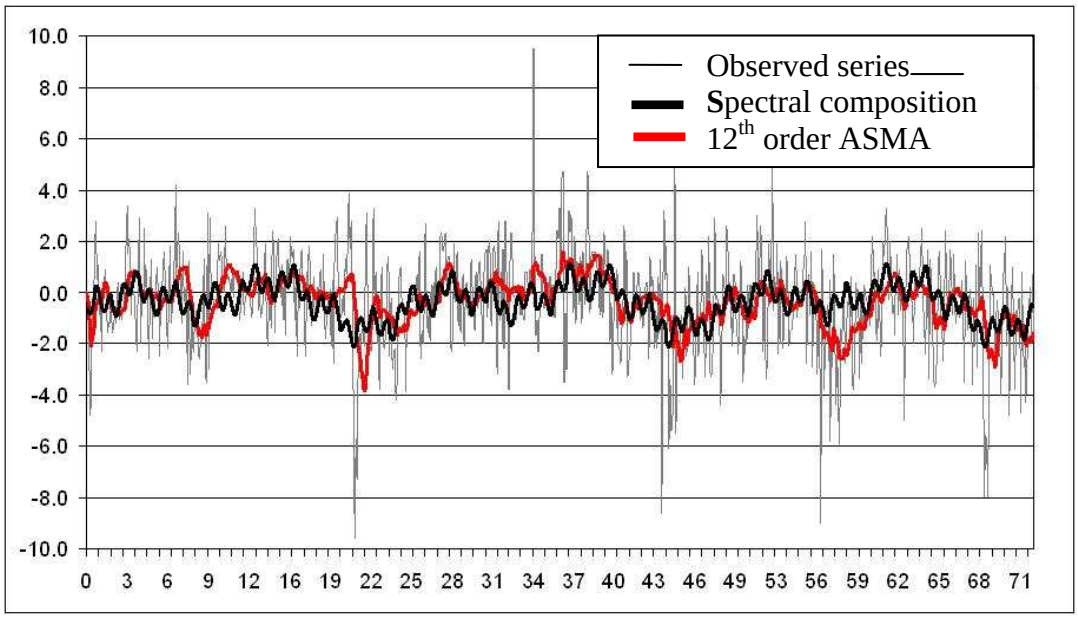

Figure 4 – Graphics of the observed North-South component changes (dN) time series, the spectral composition of the four most significant frequencies and the time series after filtering with a 12th order ASMA. The periods, in the x-axis, are in hours. The amplitudes, in the y-axis, are in mm.

The comparison of the graphic of the spectral composition to the graphic of the 12th order ASMA filtered series (Figure 4) shows differences justifiable by the criteria used in the definition of these two filters: i) The spectral composition uses the most significant frequencies, whether they are high or low; ii) The ASMA filter, as a low-pass filter, uses the low frequencies, whether they are significant or not.

7. CONCLUSIONS

The 12th order ASMA filter is adequate to remove the high frequencies and therefore is fit to smooth the observed time series as a low-pass filter. However, the 12th ASMA filter has a significant phase shift for the lower frequencies that may turn the symmetric filters a better choice, for some applications.

The experiment presented in the paper is rather a methodological exercise: further experiments over longer observation intervals, with different sampling and processing frequencies should be carried out and other kinds of filters should be experimented.

REFERENCES

Casaca, J. and Lima, J. N. (2008). *Spectral Characterization of GNSS Time Series*. 6th Luso-Spannish Assembly of Geodesy and Geophysics, Tomar.

Hamming, R. W. (1973). *Numerical Methods for Scientists and Engineers*. Dover, New York.

King, M. A., Watson, C. S., Penna, N. T. and Clarke, P. J. (2008). *Subdaily Signal in GPS Observations and Their Effect at Semiannual and Annual Periods*. Geophysical Research Letters, Vol. 35, L03302, doi: 10.1029/2007GL032252.

Mao, A., Harrison, C. and Dixon, T. (1999). *Noise in GPS Coordinate Time Series*. Journal of Geophysical Research 104 B2, 2797-2816.

Schureman, P. (1941). *Manual of Harmonic Analysis and Prediction of Tides*. U.S. Coast and Geodetic Survey, Special Publication Nº 98, Washington, D. C.

Contact of the first author

José Nuno LIMA
jnplima@lnec.pt
Division of Applied Geodesy
National Laboratory for Civil Engineering
Av. do Brasil 101, 1700-066 Lisbon
Portugal